

Structure Evolution of Volcanic Glass by Dynamic Compression

著者	Shimoda Kenji, Okuno Masayuki, Kikuchi Masae
journal or publication title	Proceedings, International Symposium of the Kanazawa University 22st-Century COE Program
volume	1
page range	387-392
year	2003-03-16
URL	http://hdl.handle.net/2297/6436

Structure Evolution of Volcanic Glass by Dynamic Compression

KEIJI SHIMODA AND MASAYUKI OKUNO

Department of Earth Science, Kanazawa University, Kanazawa, Ishikawa, 920-1192, JAPAN

MASAE KIKUCHI

Institute for Material Research, Tohoku University, Sendai, 980-8577, JAPAN

Abstract - Shock-recovery experiments have been carried out for volcanic glass with pressures up to 35GPa and the structural modifications were investigated by X-ray diffraction and Raman / infrared spectroscopy. The observed density showed maximal densification at shock pressure of ~25GPa. This densification could be attributed mainly to the reduction of T-O-T angle from Raman spectroscopic analysis. However, shock compression above 25GPa imposed density reduction. This reduction is attributed to partial annealing of the structure by high post-shock temperature. These behaviors are consistent with previous studies on other shocked glasses.

I. Introduction

The study on the structural changes of silicate glasses and crystals induced by shock-wave compression is important for understanding the formation of tektite, impactite or diaplectic glass and the estimation of shock pressure and temperature during shock events. The detailed scheme of the processes of densification and relaxation of silicate glasses through shock experiments is required in order to understand its behavior under dynamic compression precisely. Recently, several structural investigations have been performed on shock-densified SiO₂ glass [18, 23], anorthite (CaAl₂Si₂O₈) glass [21] and albite (NaAlSi₃O₈) glass [24]. These workers reported that the densification of these glasses increased rapidly with shock pressure above 15GPa and reached a maximum at about 24-26GPa before steep retrace at higher pressure and that the main mechanisms of densification were the reduction of T-O-T angle and the formation of small

rings of TO₄ tetrahedron in waste of large rings. Moreover, studies for more complex glasses will be needed to elucidate the formation of tektite which have compositional similarity to obsidian. Shock-wave equation of state for natural rhyolite was obtained by Anderson et al. [1]. Gibbons and Ahrens [4] performed shock-recovery experiment for tektite but they focused on refractive index only and insufficient pressure range up to 13GPa. In this study, the structural changes induced by shock-wave compression for natural volcanic glass (obsidian) have been analyzed using X-ray diffraction, Raman and infrared spectroscopy.

II. Experimental

A. Specimen

The specimen used in this study is a volcanic glass (obsidian) from Krafla, Iceland. This specimen is black in color and homogeneous under microscopic view. Its chemical composition are listed in Table 1. These were determined by using SEM (Topcon Alpha-30A, 20kV) with EDAX analyzer and averaged on numerous points. The calculated CIPW norm shows quartz (39.4wt%), albite (33.8wt%), orthoclase (16.6wt%), anorthite (6.5wt%), and other minerals.

B. Shock-wave experiments and density measurements

Shock-wave experiments were performed by using a single stage propellant gun (25 mm bore and 4 m length) [5] at Institute for Material Research in Tohoku University. Obsidian was cut into thin plate (10 mm in diameter, 2 mm in thickness) and encased in a stainless steel container. The specimen container was hit by a stainless steel flyer, which was accelerated to a velocity of up to about 1.6 km/s. The experiments were performed with shock pressures of 16.26, 21.74, 24.27, 30.96, and 36.79GPa. These pressures were estimated from the measured projectile velocities by using impedance matching method, with the precision of 0.1GPa.

The densities of unshocked (0.1MPa) and shock-densified obsidian were determined by suspension method in mixtures of CHI₂ and acetone. The measurements were repeated 6 times or more for each sample.

Table 1 The chemical compositions of the obsidian.

composition	wt%
SiO ₂	76.17
Al ₂ O ₃	12.27
Na ₂ O	3.99
FeO*	3.29
K ₂ O	2.82
CaO	1.69
TiO ₂	0.30
P ₂ O ₅	0.29
MnO	0.11
Cr ₂ O ₃	0.06
NiO	0.01
MgO	0.00
total	101.00

FeO* represents total iron.

C. X-ray diffraction measurements

The X-ray diffraction measurements were performed on four-circle X-ray diffractometer (Rigaku AFC-7s) with MoK α radiation monochromated by pyrolytic graphite, with the step scan technique at every 0.5° in range of 5°-120° in 2 θ , which correspond to 0.77-15.3 Å⁻¹ in $S=4\pi\sin\theta/\lambda$.

Calculation of radial distribution function was carried out by using the same procedure as Marumo and Okuno [11]. The measured X-ray scattering intensities were corrected for polarization, absorption factors, and Compton scattering factors [9]. Compton scattering factors were calculated with the analytical formulae given by Hajdu [6] and Pálinkás [19]. Normalization was carried out by Krogh-Moe's and Norman's method [8, 16]. Atomic scattering factors were taken from International Tables of X-ray Crystallography Vol. IV (1974). The composition of the obsidian used for the calculation was simplified to Na_{0.332}K_{0.154}Ca_{0.060}Fe_{0.183}Al_{0.606}Si_{3.326}O_{8.000}.

D. Raman and infrared spectroscopy

Raman spectra were recorded by using LabRamHR800 (Jobin Yvon). The 514.5 nm line (green) of Ar⁺ laser was used to excite Raman scattering, and the Raman light was collected in the back scattering geometry. All the observed Raman spectra were corrected for the temperature and frequency dependence of the first order Raman scattering [10, 14, 20].

All infrared (IR) measurements were performed by KBr micro pellet method, using FT/IR-610V (JASCO) equipped with KBr beam splitter and TGS detector. Spectra were recorded from 400cm⁻¹ to 5000cm⁻¹, with a band path of 0.96cm⁻¹.

III. Result

A. Density variations as a function of shock pressure

The density variations of obsidian with shock pressure are listed in Table 2. The densification of obsidian increases rapidly with shock pressures above ~15GPa and reaches a maximum (4.7%) at 24.27GPa, followed by rapid reduction at higher shock pressures. At 36.79GPa, the density has dropped back to almost the same density as unshocked sample.

B. X-ray diffraction analysis

X-ray scattering intensities and RDF curves are shown in Fig.1 and Fig.2, respectively. Essentially, these curves are similar in shape to each other. The broad peaks are observed at around $r=1.6$ and 3.1 Å in RDF curves. These peaks are attributed to T-O1 and T-T1 atomic pair distance (tetrahedral cation T=Si, Al), respectively. The shoulder at around 2.6 Å is assigned to O-O1 pair within a TO₄ tetrahedron, but this may include small contributions from (Na,K,Ca)-O1 pairs. Broad peaks at ~4.2 and ~5.1 Å are T-O2 and T-T2 pair

Table 2 Densities of normal and shock-compressed obsidians.

Shock pressure (GPa)	Density (g/cm ³)
unshocked	2.409(3)
16.26	2.431(3)
21.74	2.503(4)
24.27	2.522(4)
30.96	2.436(10)
36.79	2.390(4)

distance of six-membered ring, respectively [3, 7, 27, 28]. The number of oxygen atoms around a T atom was calculated to be about 4 from the area under the first peak ($r=1.63$ Å) in RDF(r) curve and the average T-O-T angle of ~149° was obtained for all samples. These facts suggest the T atoms are tetrahedrally coordinated by oxygens in the structure of both normal and shock-densified obsidian, and that no significant changes are observed on shock-densification with respect to short-range structure.

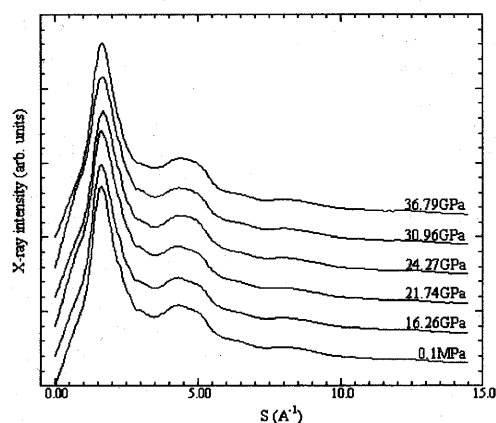


Fig.1 X-ray scattering intensities of shock-compressed obsidians

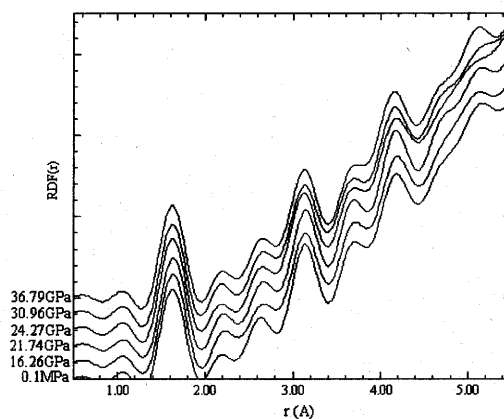


Fig.2 RDF(r) curves of shock-compressed obsidians

C. Raman and infrared spectroscopic analysis

The Raman spectra of shock-densified obsidian are shown in Fig.3. The band assignments are generally accepted as follows [12, 15, 22, 29]. Broad band centered at $\sim 490\text{cm}^{-1}$ is attributed to the bending vibration of T-O-T linkage in tetrahedral framework. This has small contribution from oxygen breathing mode of four-membered ring of TO_4 tetrahedra which generally locates at $\sim 490\text{cm}^{-1}$. The band at $\sim 800\text{cm}^{-1}$ is assigned to in-cage motion of silicon atoms in the highly polymerized network. Furthermore, the band at $1000\text{-}1200\text{cm}^{-1}$ is attributed to anti-symmetric T-O stretching vibration. The dominant peak at 670cm^{-1} can not be assigned to usual silicate glass vibration.

Fig.4 shows infrared spectra for shock-densified obsidian. There has three major bands at 460, 780, 1060cm^{-1} . The band assignments are as follows [26]. The band at around

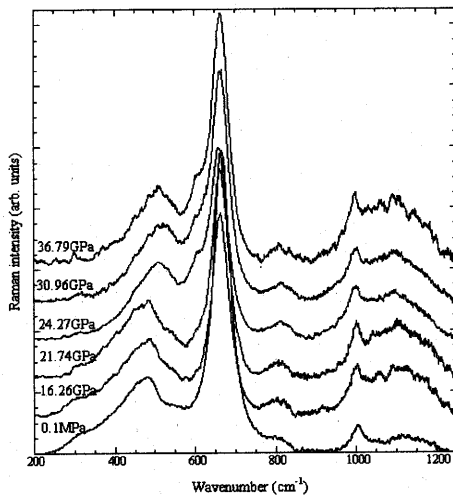


Fig.3 Raman spectra of shock-compressed obsidians

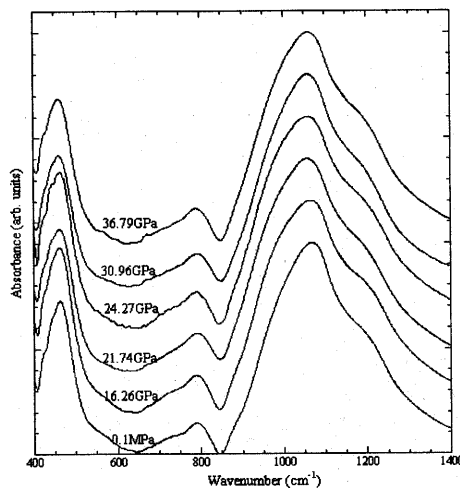


Fig.4 IR spectra of shock-compressed obsidians

460cm^{-1} is attributed to O-T-O bending vibration (deformational mode of TO_4 tetrahedron), and the bands at around $780, 1060\text{cm}^{-1}$ are assigned to T-O symmetric stretching and anti-symmetric stretching vibration, respectively.

IV. Discussion

A. Relationship between density and shock pressure

Density variations (Table 1) show the increase of densification and subsequent reduction with respect to shock pressure. This variation can be explained as follows. A first regime is that where density increases with increasing shock pressure (up to about 25GPa) due to shock compression and modest residual temperature. A second regime is that where density decreases at higher shock pressure (above 25GPa) by relaxation of densified structure due to high residual temperature [2, 18, 21].

This density variations with increasing shock pressure are similar to those of silica glass [18], anorthite glass [21] and albite glass [24]. The maximal densification for shock-densified silica glass, anorthite glass, and albite glass is 11.0%, 2.2%, and 4.2%, respectively at shock pressure of 24-26GPa. This differences in maximal densification must be due to the differences in the original glass structure [21]. Taylor and Brown reported that albite glass has "stuffed tridymite-like" structure constituted of six-membered rings of TO_4 tetrahedra, in which modifier cation, Na is interstitial, and that anorthite glass is represented as feldspar structure constituted of four-membered rings [11, 25]. These results explain why the maximal densifications of albite and anorthite glass are smaller than silica glass. Considering the chemical composition of obsidian (Table 1), maximal densification of 4.7% is qualitatively consistent with previous studies mentioned above.

B. Structural evolution in shock-densified obsidian

As mentioned before, RDF curves calculated from X-ray scattering intensities are similar in shape to each other (Fig.2) and they indicate that normal and shock-densified obsidian have TO_4 tetrahedra as a basic structural unit. In addition, the presence of the peak at about 5.1 \AA means that six-membered ring is predominant in obsidian structure, and it is consistent with the results on other rhyolitic glasses [7, 17]. However, no clear modifications are observed with increasing shock pressure in RDF curves. It is well known that in shock-recovery experiments (or even static condition) highly-coordinated silicon species created during shock-propagation can not be quenched on shock release and revert to tetrahedral one. This fact is supported by our preliminary check by NMR spectra, which show only tetrahedral silicon species. Therefore, structural changes on shock densification could not be well analyzed from RDF analysis.

Recently, structural evolutions for several silicate glasses have been reported, as a function of pressure or composition,

in terms of FSDP (First Sharp Diffraction Peak) which corresponds to first peak of X-ray diffraction profile. Shimada et al. [23] reported that the FSDP for shock-densified SiO₂ glass moved with increasing pressure, correspondent to density variation. Table 3 shows the variations of FSDP position for shock-densified obsidian. Our result also indicate that FSDP moves to higher *S* values with shock pressure up to ~25GPa and retraces to lower values with higher pressure. Some workers such as Shimada et al. [23] and Susman et al. [30] have related FSDP position to medium-range structure, especially to the distribution of ring statistics. They insisted migration of FSDP to higher value with pressure indicating the augmentation on the population of small rings as 3-, or 4-membered ring. Therefore, we can suggest that small rings increase with applied shock pressure up to ~25GPa but decrease at higher pressures because of the relaxation of these rings due to high post-shock temperature.

Raman spectra for shock-compressed obsidian show clear pressure variations. The frequency of the broad band at around 490cm⁻¹ show positive shifts (~21cm⁻¹) from 483cm⁻¹ to 504cm⁻¹ with increasing shock pressure up to 30.96GPa, and subsequent reduction to 495cm⁻¹ at 36.79GPa (Fig.5) with large deviations. This band is attributable to T-O-T bending mode of TO₄ network structure. Thus, this band is related to average T-O-T angle, and positive frequency shift with shock pressure means the reduction of average T-O-T angle [13, 14]. Corresponding band shift for shock-densified silica glass reported by Okuno et al. is 48 cm⁻¹ (457cm⁻¹ to 505cm⁻¹) [18]. This difference in frequency shift between shock-densified obsidian and SiO₂ glass may correspond to the difference in maximal densification (4.7% for obsidian versus 11.0% for silica glass). But, it should be noted that the frequency variations of this T-O-T bending mode (maximum at ~30GPa) do not seem to be strictly correlated to density variations (maximum at ~25GPa) for shock-densified obsidian. This fact is also reported by Okuno et al. [18]. They also gave a result for the variations of Raman frequency and intensity for SiO₂ glass compressed at 26.31GPa as a function of annealing temperature, and observed that Si-O-Si bending mode started to relax at lower temperature than the intensity of 3-membered rings does [18]. From this observation we can say that T-O-T bond angle readily relax at low post-shock temperature but 3- or 4-membered rings retain until at higher temperature attained at higher shock pressure, and that apparent maximum of T-O-T bending mode at 30.96GPa occurs due to overlap

Table 3 FSDP positions of shock-compressed obsidians

Shock pressure (GPa)	FSDP position (Å ⁻¹)
unshocked	1.6870
16.26	1.6980
21.74	1.7310
24.27	1.7655
30.96	1.7470
36.79	1.7090

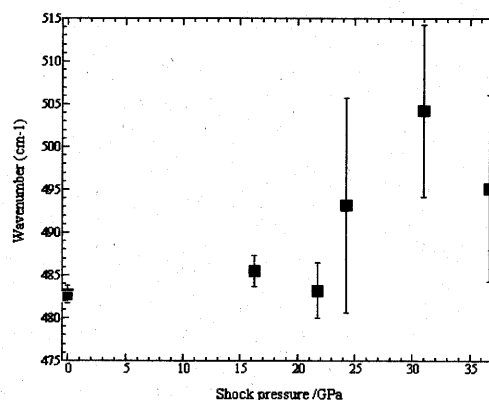


Fig.5 Frequency variations of the broad 490cm⁻¹ band in Raman spectra as a function of shock pressure

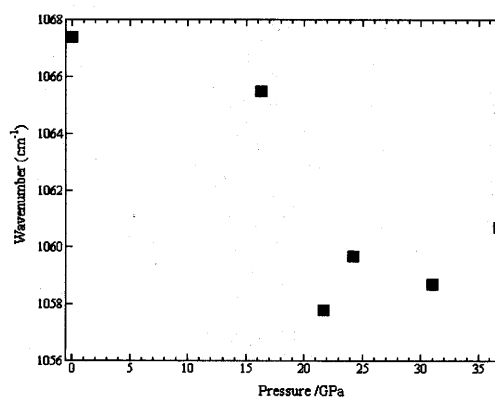


Fig.6 Frequency variations of the T-O stretching vibration centered at 1060 cm⁻¹ in IR spectra

with the breathing mode of 4-membered rings.

The band at ~1060 cm⁻¹ in IR spectra, which is attributed to T-O anti-symmetric stretching, shifts to lower frequency with increasing shock pressure of 20-30GPa (Fig.6). This indicates slight lengthening of Si-O bond distance, and gives indirect suggestion of the reduction of mean T-O-T angle.

From these results and discussion, the densification mechanism of obsidian during shock compression is considered as follows.

- 1) Up to shock pressure of ~25GPa, the densification is mainly caused by reduction of average T-O-T angle that is attributed to shrinkage of the framework structure of TO₄ tetrahedra and increase of small rings of TO₄ tetrahedra .
- 2) Above ~25GPa, high residual temperature may cause the relaxation of compressed TO₄ tetrahedral network, i.e., re-increasing average T-O-T bond angle and slight relaxation of small rings. These result in density reduction.

Pressure-induced evolution of crystallites

The 670cm^{-1} band in Raman spectra for natural obsidian is prominent (Fig.3). This band does not exist in the spectra of fused glass [31], nor the other silicate glasses such as silica glass, albite glass, and anorthite glass [18, 21, 24, etc.]. This band could be attributed to crystallite [17]. The intensity of this band seems to decrease with shock pressure above 25-30GPa, but the extent to which differ from point to point ($\sim 2\mu\text{m}$) for which we accumulated spectra.

To investigate the pressure-induced changes in the relative quantity of crystallites in more averaged scale, powder X-ray diffraction measurements are also performed with $\text{CuK}\alpha$ radiation (Fig.7). The X-ray diffraction patterns for shocked obsidian have broad peak at around $2\theta = 23^\circ$, which is due to glass matrix in the obsidian structure. There are two more prominent sharp peaks positioned at $2\theta = 29.9^\circ$ and 35.1° , which could be assigned to crystallites. These peaks are not observed in the diffraction pattern for fused glass [31]. Figure 7 shows the intensity reduction of these two peaks as a function of shock pressure above $\sim 25\text{GPa}$. From these results, it is concluded that crystallites in this obsidian begin to amorphize with shock pressure above 25GPa.

V. Conclusions

The structural evolutions of obsidian by shock-wave compression can be summarized as follows.

For shock pressure up to about 25GPa, the density of obsidian increases with increasing shock pressure. The maximal densification of 4.7% are obtained for the obsidian. This is roughly intermediate between the ones for silica and feldspar glasses. This reflects their structural differences.

Pressure variations in Raman spectra indicate that the densification for shock pressure up to about 25GPa is due to the reduction of average T-O-T angle, with small contribution from the increase of the population of small rings (such as 3-, 4-membered ring).

Above $\sim 25\text{GPa}$, the density decreases with increasing shock pressure. This may be due to partial relaxation of densified structure by relatively high residual temperature

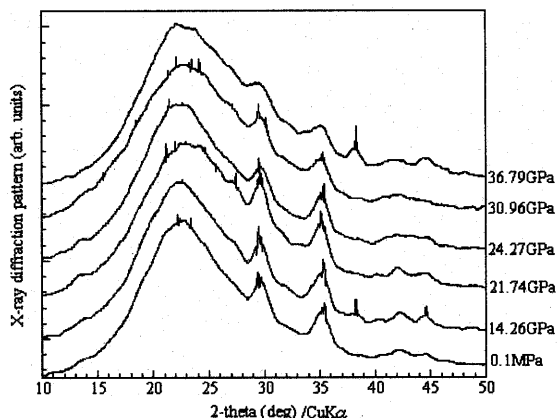


Fig7 X-ray diffraction patterns ($\text{CuK}\alpha$) of shock-compressed obsidians

after shock-wave compression. Furthermore, it is found that crystallites start to amorphize with shock pressure above 25GPa.

Acknowledgements

I would like to acknowledge Dr. Bruno Reynard of ENS Lyon for providing obsidian blocks. I also wish to express my thanks to Mr. Shoichi Okamoto of Horiba Jovin Yvon Co., Ltd. and Dr. Mikio Koyano of JAIST for carrying out Raman spectra measurements. A part of this study was carried out under the Visiting Researcher's Program of the IMR, Tohoku University, Japan.

References

- [1] W. W. Anderson, W. Yang, G. Chen and T. J. Ahrens, "Shock-wave equation of state of rhyolite", *Geophys J Int* Vol. 132, pp. 1-13, 1998.
- [2] J. Arndt, H. Hornemann and W. F. Müller, "Shock-wave densification of silica glass", *Phys Chem Glasses* Vol. 12, pp.1-7, 1971.
- [3] G. E. Brown, F. Farges and G. Calas, "X-ray scattering and X-ray spectroscopy studies of silicate melts", In: J. F. Stebbins, P. F. McMillan and D. B. Dingwell (ed), *Structure, dynamics and properties of silicate melts -Reviews in Mineralogy* Vol. 32 MSA, Washington D.C., pp. 317-410, 1995.
- [4] R. V. Gibbons and T. J. Ahrens, "Shock metamorphism of silicate glasses", *J Geophys Res*, Vol.76, pp. 5489-5498, 1971.
- [5] T. Goto and Y. Syono, "Technical aspect of shock compression experiments using the gun method", In: I. Sunagawa (ed), *Material sciences of the earth's interior*. Terra Scientific Publ Co., Tokyo, pp. 605-619, 1984.
- [6] F. Hadju, "Analytic approximation for incoherent scattered X-ray intensities", *Acta Cryst* A27, pp. 73-74, 1971.
- [7] M. F. Hochella and G. E. Jr. Brown, "Structure and viscosity of rhyolitic composition melts", *Geochim Cosmochim Acta* Vol. 48, pp. 2631-2640, 1984.
- [8] J. Krogh-Moe, "A method for converting experimental X-ray intensities to an absolute scale", *Acta Cryst* Vol. 9, pp. 951-953, 1956.
- [9] H. A. Levy, M. D. Danford and A. H. Narten, "Data collection and evaluation with an X-ray diffractometer designed for the study of liquid structure", Oak Ridge National Laboratory Report 3960, 1966.
- [10] D. A. Long, "Raman spectroscopy", McGraw Hill, 1977.
- [11] F. Marumo and M. Okuno, "X-ray structural studies of molten silicates: Anorthite and albite melts", In: I. Sunagawa (ed), *Material sciences of the earth's interior*. Terra Scientific Publ Co., Tokyo, pp. 25-38, 1984.
- [12] P. McMillan, "Structural studies of silicate glasses and melts: applications and limitation of Raman spectroscopy", *Am Mineral* Vol. 69, pp. 622-644, 1984.
- [13] P. McMillan, B. Piriou and R. Couty, "A Raman study

- of pressure-densified vitreous silica”, *J Chem Phys* Vol. 81, pp. 4234-4236, 1984.
- [14] P. F. McMillan and G. H. Wolf, “Vibrational spectroscopy of silicate liquids”, In: J. F. Stebbins, P. F. McMillan and D. B. Dingwell (ed), *Structure, dynamics and properties of silicate melts – Reviews in Mineralogy* Vol. 32 MSA, Washington DC, pp. 247-315, 1995.
- [15] B. O. Mysen, D. Virgo and A. Seifert, “The structure of silicate melts: implications for chemical and physical properties of natural magma”, *Rev Geophys Space Phys* Vol. 20, pp. 353-383, 1982.
- [16] N. Norman, “A Fourier transformation method for normalizing intensities”, *Acta Cryst* Vol. 12, pp. 370-374, 1957.
- [17] M. Okuno, S. Nakagami, Y. Shimada, K. Kusaba, Y. Syono, N. Ishizawa and H. Yusa, “Structural changes of a volcanic glass (obsidian) under high pressure”, *Rev High Pressure Sci Technol* Vol. 7, pp. 128-130, 1998.
- [18] M. Okuno, B. Reynard, Y. Shimada, Y. Syono and C. Williams, “A Raman spectroscopic study of shock-wave densification of vitreous silica”, *Phys Chem Minerals* Vol. 26, pp. 304-311, 1999.
- [19] G. Pálinkás, “Analytic approximation for the incoherent X-ray intensities of atoms Ca to Am”, *Acta Cryst* A29, pp. 10-12, 1973.
- [20] B. Piriou and D. Alain, “Density states and structural form related structural properties of amorphous solids”, *High Temp High Press Res* Vol. 11, pp. 407-414, 1979.
- [21] B. Reynard, M. Okuno, Y. Shimada, Y. Syono and C. Williams, “A Raman spectroscopic study of shock-wave densification of anorthite ($\text{CaAl}_2\text{Si}_2\text{O}_8$) glass”, *Phys Chem Minerals* Vol. 26, pp. 432-436, 1999.
- [22] F. A. Seifert, B. O. Mysen, D. Virgo, “Three-dimensional network structure of quenched melts (glass) in system $\text{SiO}_2\text{-NaAlO}_2$, $\text{SiO}_2\text{-CaAl}_2\text{O}_4$ and $\text{SiO}_2\text{-MgAl}_2\text{O}_4$. *Am Mineral* 67, 696-717, 1982.
- [23] Y. Shimada, M. Okuno, Y. Syono, M. Kikuchi, K. Fukuoka and N. Ishizawa, “An X-ray diffraction study of shock-wave-densified SiO_2 glasses”, *Phys Chem Minerals* Vol. 29, pp. 233-239, 2002.
- [24] K. Takabatake, “Vitrification of albite crystal and structure change of albite glass by shock-wave compression”, master thesis of Kanazawa University, 2000.
- [25] M. Taylor and G. E. Jr. Brown, “Structure of mineral glasses – I. The feldspar glasses $\text{NaAlSi}_3\text{O}_8$, KAlSi_3O_8 , $\text{CaAl}_2\text{Si}_2\text{O}_8$ ”, *Geochim Cosmochim Acta* Vol. 43, pp. 61-75, 1979a.
- [26] B. Velde and R. Couty, “High pressure infrared spectra of some silicate glasses”, *Chem Geol* Vol. 62, pp. 35-41, 1987.
- [27] G. H. Wolf and P. F. McMillan, “Pressure effects on silicate melt: Structure and properties”, In: J. F. Stebbins, P. F. McMillan and D. B. Dingwell (ed), *Structure, dynamics and properties of silicate melts – Reviews in Mineralogy* Vol. 32 MSA, Washington DC, pp. 505-561, 1995.
- [28] N. Zotov, V. Dimitoriv and Y. Yanev, “X-ray radial distribution function analysis of acid volcanic glasses from the Eastern Rhodopes, Bulgaria”, *Phys Chem Minerals* Vol. 16, pp. 774-782, 1989.
- [29] N. Zotov, Y. Yanev, M. Epelbaum and L. Konstantinov, “Effect of water on the structure of rhyolite glasses – X-ray diffraction and Raman spectroscopy studies”, *J Non-Cryst Solids* Vol. 142, pp. 234-246, 1992.
- [30] S. Susman, K. J. Volin, R. C. Liebermann, G. D. Gwanmesia and Y. Wang, “Structural changes in irreversibly densified fused silica: implications for the chemical resistance of high-level nuclear waste glasses”, *Phys Chem Glasses* Vol. 31, pp. 144-150, 1990.
- [31] K. Shimoda, “Structural changes of an obsidian and its fused glass by shock-wave compression”, master thesis of Kanazawa University, 2001.